ISIJ International, Vol. 53 (2013), No. 1, pp. 76–80

High-Performance Prediction of Molten Steel Temperature in Tundish through Gray-Box Model

Toshinori OKURA,[1)] Iftikhar AHMAD,[1)] Manabu KANO,[2)]* Shinji HASEBE,[1)] Hiroshi KITADA[3)] and Noboru MURATA[4)]

1) Dept. of Chemical Engineering, Kyoto University, Nishikyo-ku, Kyoto, 615-8510 Japan.
2) Dept. of Systems Science, Kyoto University, Yoshida-Honmachi, Sakyo-ku, Kyoto, 606-8501 Japan.
3) Sumitomo Metal Industries, Ltd., 1-8 Fusocho, Amagasaki-shi, Hyogo, 660-0891 Japan.
4) Dept. of Electrical Engineering and Bioscience, Waseda University, 3-4-1 Okubo, Shinjuku-ku, Tokyo, 169-8555 Japan.

(*Received on July 30, 2012; accepted on August 31, 2012*)

A novel gray-box model is proposed to estimate molten steel temperature in a continuous casting process at a steel making plant by combining a first-principle model and a statistical model. The first-principle model was developed on the basis of computational fluid dynamics (CFD) simulations to simplify the model and to improve estimation accuracy. Since the derived first-principle model was not able to estimate the molten steel temperature in the tundish with sufficient accuracy, statistical models were developed to estimate the estimation errors of the first-principle model through partial least squares (PLS) and random forest (RF). As a result of comparing the three models, *i.e.*, the first-principle model, the PLS-based gray-box model, and the RF-based gray-box model, the RF-based gray-box model achieved the best estimation performance. Thus, the molten steel temperature in the tundish can be estimated with accuracy by adding estimates of the first-principle model and those of the statistical RF model. The proposed gray-box model was applied to the real process data and the results demonstrated its advantage over other models.

KEY WORDS: gray-box modeling; steel making process; soft-sensor; virtual sensing.

1. Introduction

The steel industry faces a stiff competition in the global market, and each steel company has to produce high quality products satisfying various customer demand. A key issue is to realize stable operation and high productivity.[1)] For example, a breakout may occur in the worst case if molten steel temperature is not controlled precisely in a continuous casting process. Breakouts cause tremendous increase in maintenance cost and productivity loss. Hence, in the steel making process, whose diagram is shown in **Fig. 1**, molten steel temperature in the tundish (TD temp) is one of key factors to realize stable operation and high productivity. However, no effective manipulated variable is available in the continuous casting process to control TD temp. To realize precise control of TD temp, it is necessary to adjust the molten steel temperature in the Ruhrstahl-Heraeus process at the end of its operation (RH temp). Thus, a model relating TD temp and RH temp needs to be constructed. The modeling is difficult because various factors, *e.g.* degradation of ladles and various treating time at each station, affect molten steel temperature in the ladle and the tundish.

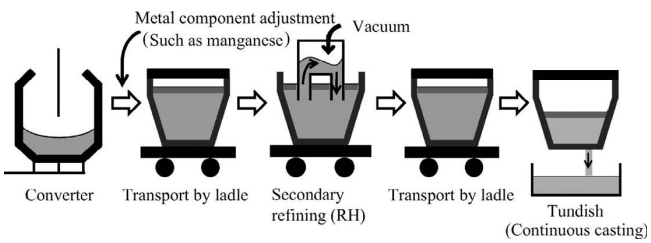

Fig. 1. Process flow diagram of the steel making process.

In the past, various models such as first-principle models,[2–7)] statistical models,[8)] and gray-box models[9)] have been proposed. The first-principle models include one dimensional models[2,3)] and computational fluid dynamics (CFD) models.[4–7)] In general, one-dimensional models are too simple to predict TD temp precisely, and CFD-based models are too complicated and thus spend much computational time. On the other hand, it is difficult to achieve sufficient estimation accuracy by using statistical models without utilizing process knowledge from limited samples. The gray-box model,[9)] which integrated a first-principle model and a statistical model, attains better results and spends less computational time.

In the present work, a novel gray-box model is proposed. First, a first-principle model is developed for a transportation period from the secondary refining to the continuous casting and for a casting period. This model takes account of heat balance among molten steel, slag, air, ladle, and tundish. The results of CFD analysis[4)] are used to simplify the model and to achieve high estimation performance. Then, statistical models are developed by considering all the process shown in Fig. 1, in order to compensate the estima-

* Corresponding author: E-mail: manabu@human.sys.i.kyoto-u.ac.jp
DOI: http://dx.doi.org/10.2355/isijinternational.53.76

tion error of the first-principle model. The statistical models are built through partial least squares (PLS) and random forest (RF). Finally, the first-principle model and the statistical models are integrated into gray-box models. The derived models, *i.e.*, the first principle model, the statistical models, and the gray-box models, are compared in the estimation performance.

2. First-Principle Model

In this section, the proposed first-principle model to estimate TD temp is explained. This first-principle model consists of two parts; the first one models phenomena during the transportation period from the secondary refining to the continuous casting, and the other one models phenomena during the casting period. In this model, the degradation of ladles needs to be taken into account.

2.1. First-Principle Model for Transportation Period

2.1.1. Molten Steel in Ladle

It is assumed that the ladle is a cylinder of radius R_i. CFD simulation results have indicated that thermal stratification is formed vertically in the standing ladle due to natural convection.[4] The thermal stratification affects TD temp directly; thus it needs to be modeled. In this work, on the basis of the CFD results, the molten steel temperature is modeled as a function of time t and position z from the bottom of the ladle:

$$T_m(z,t) = \bar{T}_m(t) + k(t)\left(\sqrt{\frac{z}{H_m}} - \frac{2}{3}\right) \quad \text{..... (1)}$$

where T_m is the molten steel temperature, $\bar{T}_m$ is the average molten steel temperature, k denotes the difference between the molten steel temperature at the top and the bottom of the ladle, and H_m is the depth of the molten steel in the ladle.

The results of CFD simulations have shown that the temperature difference is a function of time,[4] thus it is modeled with parameter a:

$$k(t) = at \quad \text{..... (2)}$$

The method of calculating the time evolution of the molten steel temperature T_m is shown in **Fig. 2**. First, the average molten steel temperature $\bar{T}_m(t+\Delta t)$ is calculated through the heat balance equation:

$$\begin{aligned}\rho_m c_m \pi R_i^2 H_m \frac{d\bar{T}_m(t)}{dt} = &-2\pi R_i \int_0^{H_m} U_w (T_m(z,t) - T_{am})dz \\ &-\pi R_i^2 U_b (T_m(0,t) - T_{am}) \\ &-\pi R_i^2 h_1 (T_m(H_m,t) - T_{sl}(t))\end{aligned} \quad \text{... (3)}$$

where ρ_m and c_m are the density and the heat capacity of the molten steel, respectively. U_b and U_w are the overall heat transfer coefficients of the ladle bottom and the ladle wall, respectively. T_{am} and T_{sl} are the ambient temperature and the slag temperature, respectively. In addition, h_1 denotes the heat transfer coefficient between the molten steel and the slag. The left side of Eq. (3) represents the time change of the molten steel enthalpy. The first, second, and third terms of the right side represent the heat conduction from the molten steel to the ladle wall, to the ladle bottom, and to the slag, respectively. The initial molten steel temperature is assumed to be homogenous and the same as RH temp because the molten steel in the ladle is properly stirred. The temperature difference between the top and the bottom is calculated through Eq. (2).

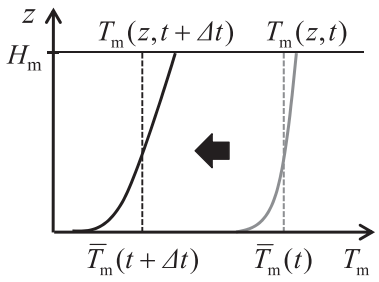

Fig. 2. Update of molten steel temperature in ladle T_m.

2.1.2. Slag in Ladle

Slag in the standing ladle, which is generated in the convertor, keeps the molten steel at high temperature. The heat balance of the slag is modeled as a lumped parameter system.

$$\begin{aligned}\rho_{sl} c_{sl} \pi R_i^2 H_{sl} \frac{dT_{sl}(t)}{dt} = &\pi R_i^2 h_1 (T_m(H_m,t) - T_{sl}(t)) \\ &-\pi R_i^2 \varepsilon_{sl-lin} \sigma (T_{sl}(t)^4 - T_{a1}^4) \\ &-\pi R_i^2 h_2 (T_{sl}(t) - T_{a1}) \\ &-2\pi R_i H_{sl} U_w (T_{sl}(t) - T_{am})\end{aligned} \quad \text{.... (4)}$$

where ρ_{sl}, c_{sl}, and ε_{sl-lin} are the density, the heat capacity, and the emissivity of the slag, respectively. H_{sl} denotes the slag layer thickness, h_2 the heat transfer coefficient between the slag and the air in the ladle, T_{a1} the air temperature in the ladle, and σ the Stefan-Boltzmann coefficient. The left side of Eq. (4) represents the time change of the slag enthalpy. The first, second, third and fourth terms of the right side represent the heat conduction from the molten steel to the slag, the radiation from the slag to the ladle cover, the heat conduction from the slag to the air in the ladle, and that from the slag to the ladle wall, respectively. The ladle wall temperature, which affects the radiation, is assumed to be equal to the air temperature.

2.1.3. Ladle Degradation

Ladles are used repeatedly for transportation of molten steel and degrade gradually. The CFD simulations have indicated that if the ladle degrades, the temperature difference between the top and the bottom, the molten steel temperature and the heat conduction flux from the molten steel to the external environment increase. In the proposed first-principle model, it is assumed that the increase of the heat flux corresponds to the increase of overall heat transfer coefficients of the ladle U_w and U_b, and the increase in temperature difference corresponds to the increase of parameter a in Eq. (2). These parameters are described as functions of the number of usage n. $U_w(n)$ is expressed in terms of $U_b(n)$ for simplicity.

$$U_w(n) = \eta U_b(n) \quad \text{..... (5)}$$

$$U_b(n) = U_{b0} + \alpha\sqrt{n} \quad \text{..... (6)}$$

$$a(n) = a_0 + \beta\sqrt{n} \quad \text{..... (7)}$$

where U_{b0}, a_0, α, β, and η are constants.

2.2. First-Principle Model for Casting Period

2.2.1. Molten Steel in Ladle

It is assumed that volumetric flow Q from the ladle to the tundish is constant and the depth of the molten steel in the ladle decreases by ΔH_m during Δt. In addition, the outflow temperature is assumed to be the average temperature $T_{in}(t)$ within $0 \le z \le \Delta H_m$. It is also assumed that the increase of the temperature difference $k(t)$ stops at the end of transportation period. On the other hand, the heat radiation continues and $T_m(t)$ decreases to $T_m(t + \Delta t)$. This decrease in $T_m(t)$ corresponds to the parallel shift from $T_m(z, t)$ to $T_m(z, t + \Delta t)$: $-\Delta H_m$ in z axial direction and $\Delta \overline{T}_m$ in T_m axial direction as shown in **Fig. 3**. The $T_m(z, t)$ distributes over the following region:

$$-\frac{Q}{\pi R_i^2}(t-t_1) \le z \le H_m - \frac{Q}{\pi R_i^2}(t-t_1) \quad \text{..... (8)}$$

where t_1 is the time at the end of transportation.

2.2.2. Molten Steel in Tundish

It is assumed that the inflow to the tundish is equal to the outflow from the tundish and also the depth of the molten steel in the tundish is constant. The CFD simulations have indicated that TD temp is distributed in the flow direction.[10] Thus, in this work, the tundish is modeled as a compartment model consisting of N_t isothermal baths connected in series as shown in **Fig. 4**. The heat balance of the k-th bath is

$$\begin{aligned}\rho_m c_m WH \frac{L}{N_t}\frac{dT_t^{(k)}(t)}{dt} &= \rho_m c_m Q T_t^{(k-1)}(t) - \rho_m c_m Q T_t^{(k)}(t) \\ &\quad - S_t U_t (T_t^{(k)}(t) - T_{am}) \\ &\quad - W\frac{L}{N_t}\varepsilon_{mol-lin}\sigma(T_t^{(k)}(t)^4 - T_{a2}^4) \\ &\quad - W\frac{L}{N_t}h_3(T_t^{(k)}(t) - T_{a2})\end{aligned} \quad \text{... (9)}$$

$$S_t = \begin{cases} W\dfrac{L}{N_t} + 2H\dfrac{L}{N_t} + WH & (k = 1, N_t) \\ W\dfrac{L}{N_t} + 2H\dfrac{L}{N_t} & (k = 2, 3, \cdots, N_t - 1) \end{cases} \quad \text{..... (10)}$$

where W, H, and L denote the width, the height, and the length of molten steel in the tundish, respectively. $T_t^{(k)}$ is TD temp in the k-th bath. S_t denotes the contact area between the molten steel and the tundish, U_t the overall heat transfer coefficient of the tundish, $\varepsilon_{mol-lin}$ the emissivity of the molten steel, and h_3 the heat transfer coefficient between the molten steel and the air. $T_t^{(0)}(t)$ is equal to $T_{in}(t)$ because the molten steel poured from the ladle flows into the first bath. The left side of Eq. (9) represents the time change of the molten steel enthalpy. The first to fifth terms of the right side represent the inflow enthalpy, outflow enthalpy, conduction from the molten steel to the tundish wall, radiation from the molten steel, and conduction from the molten steel to the air in the tundish, respectively. The tundish wall temperature is assumed to be equal to the air temperature T_{a2}, which is assumed to be constant. In this study, the influence of former batch on the measurement of TD temp is assumed to be negligible.

2.2.3. Parameter Fitting and Model Validation

The first-principle model contains ten parameters to be identified, *i.e.*, a_0, h_1, h_2, h_3, T_{a1}, T_{a2}, U_{b0}, U_t, α, and β. These parameters were estimated through least squares algorithm using real process data provided by Sumitomo Metal Industries, Ltd. in Japan. A total of 1 155 samples were used for parameter estimation. The input variables of the first-principle model were the number of ladle usage, the weight of the molten steel, RH temp, transportation time, and casting time. The output variable, TD temp, was scaled not to reveal its real value.

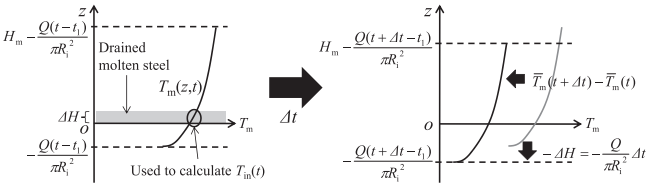

Fig. 3. Model of molten steel temperature in ladle during the casting period.

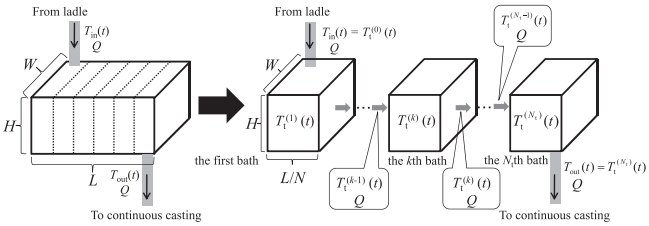

Fig. 4. Compartment model of molten steel in tundish.

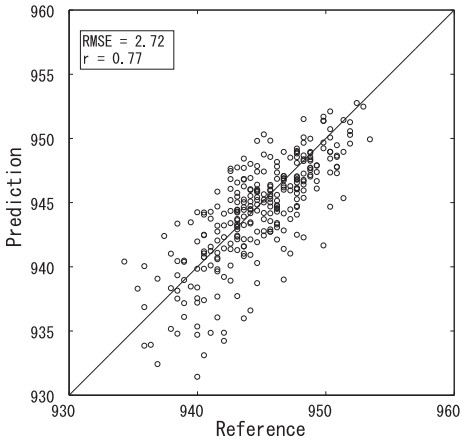

Fig. 5. Prediction of TD temp through the first-principle model.

The developed model was validated by using 289 samples, which were used only for validation. The prediction result through the first-principle model is shown in **Fig. 5**. The prediction performance was evaluated on the basis of the root-mean-square error (RMSE) and the correlation coefficient between reference (measured values) and predicted values (r). RMSE of scaled TD temp was 2.72, which did not meet our specification. Hence, the prediction performance of the developed first-principle model was not sufficient for its industrial application.

3. Gray-Box Model

To improve the prediction performance, the developed first-principle model can be integrated with a statistical model. Such an integration derives a gray-box model.

In the proposed gray-box modeling method, TD temp T_{TD} is predicted through the first-principle model f_{fp} and then the error e is predicted through a statistical model f_{st}. In other words, TD temp is predicted by adding the output of the first-principle model and that of the statistical model.

$$\hat{T}_{fp} = f_{fp}(T_{RH}, \boldsymbol{x}_{fp}) \quad \text{..... (11)}$$

$$e = T_{TD} - \hat{T}_{fp} \quad \text{..... (12)}$$

$$\hat{e} = f_{st}(\boldsymbol{x}_{st}) \quad \text{..... (13)}$$

$$\hat{T}_{TD} = \hat{T}_{fp} + \hat{e} \quad \text{..... (14)}$$

where $\hat{T}_{fp}$ denotes TD temp predicted through the first-principle model. RH temp T_{RH} and $\boldsymbol{x}_{fp}$ are input variables for the first-principle model. $\boldsymbol{x}_{st}$ is input variables for the statistical model, whose output is the predicted error $\hat{e}$; it includes measured variables of processes from the converter to the tundish because not only processes from the secondary refining to the tundish but also processes from the convertor to the secondary refining affect TD temp.

In this section, statistical modeling methods, *i.e.*, PLS and RF, are briefly explained. Then gray-box models are constructed and compared with other models in the prediction performance.

3.1. Partial Least Squares (PLS)

PLS is a linear regression method that can cope with the collinearity problem; thus it has been used as a modeling tool in various industries where process variables are highly correlated.[11)]

In PLS with one output variable, input data $\boldsymbol{X} \in \Re^{N \times M}$ and output data $\boldsymbol{y} \in \Re^{N}$ are decomposed as follows:

$$\boldsymbol{X} = \boldsymbol{T}\boldsymbol{P}^T + \boldsymbol{E} \quad \text{..... (15)}$$

$$\boldsymbol{y} = \boldsymbol{T}\boldsymbol{b} + \boldsymbol{f} \quad \text{..... (16)}$$

where $\boldsymbol{T} \in \Re^{N \times R}$ is a latent variable matrix whose columns are latent variables $\boldsymbol{t}_r \in \Re^{N}$ $(r = 1, 2, \cdots, R)$, $\boldsymbol{P} \in \Re^{M \times R}$ is a loading matrix of $\boldsymbol{X}$ and its columns are loading vectors $\boldsymbol{p}_r$, $\boldsymbol{b} = [b_1, b_2, \cdots, b_R]^T$ is a loading vector of $\boldsymbol{y}$, and $\boldsymbol{E}$ and $\boldsymbol{f}$ are errors. N, M, and R denote the number of samples, that of input variables, and that of adopted latent variables, respectively.

The nonlinear iterative partial least squares (NIPALS) algorithm can be used to construct the PLS model. Suppose that the first to $(r-1)$th latent variables $\boldsymbol{t}_1, \boldsymbol{t}_2, \cdots, \boldsymbol{t}_{r-1}$, the loading vectors $\boldsymbol{p}_1, \boldsymbol{p}_2, \cdots, \boldsymbol{p}_{r-1}$ and $b_1, b_2, \cdots, b_{r-1}$ are given. The rth residual input and output can be written as follows:

$$\boldsymbol{X}_r = \boldsymbol{X}_{r-1} - \boldsymbol{t}_{r-1}\boldsymbol{p}_{r-1}^T \quad \text{..... (17)}$$

$$\boldsymbol{y}_r = \boldsymbol{y}_{r-1} - b_{r-1}\boldsymbol{t}_{r-1} \quad \text{..... (18)}$$

where $\boldsymbol{X}_1 = \boldsymbol{X}$ and $\boldsymbol{y}_1 = \boldsymbol{y}$. The latent variable $\boldsymbol{t}_r$ is a linear combination of the columns of $\boldsymbol{X}_r$, that is, $\boldsymbol{t}_r = \boldsymbol{X}_r\boldsymbol{w}_r$ where $\boldsymbol{w}_r \in \Re^{M}$ is the rth weighting vector. PLS aims to maximize the covariance between $\boldsymbol{y}_r$ and $\boldsymbol{t}_r$ under the constraint $\| \boldsymbol{w}_r \| = 1$. By using the Lagrange multipliers method, $\boldsymbol{w}_r$ is derived as

$$\boldsymbol{w}_r = \frac{\boldsymbol{X}_r^T \boldsymbol{y}_r}{\| \boldsymbol{X}_r^T \boldsymbol{y}_r \|}. \quad \text{..... (19)}$$

The rth loading $\boldsymbol{p}_r$ and b_r are as follows:

$$\boldsymbol{p}_r = \frac{\boldsymbol{X}_r^T \boldsymbol{t}_r}{\boldsymbol{t}_r^T \boldsymbol{t}_r} \quad \text{..... (20)}$$

$$b_r = \frac{\boldsymbol{y}_r^T \boldsymbol{t}_r}{\boldsymbol{t}_r^T \boldsymbol{t}_r}. \quad \text{..... (21)}$$

Finally, the above procedure is repeated until the number of adopted latent variables R is achieved; R can be determined by some cross validation technique.[12,13)] In cross validation, training data is divided into several subgroups. PLS models are constructed iteratively. At each iteration, one subgroup is used for model validation and the other subgroups are used for model construction. On the basis of the sum of prediction errors, the optimal number of latent variables adopted in the PLS model is determined.

3.2. Random Forest (RF)

RF is an ensemble classifier that consists of many decision trees.[14)] RF combines Breiman's bagging idea and the random selection of split features.[15,16)] Bagging is a mechanism to improve stability and accuracy of classification and regression models. Given a training set D of size N, bagging generates M new training sets D_m^* (m = 1, 2, $\cdots$, M), whose size is N, by random sampling from D with replacement. The set D_m^* expected to have 63.2% of the unique datasets in D and the rest is duplicated. The newly created training datasets are called bootstrapped samples while the fraction of original data that is not bootstrapped is termed out-of-bag (OOB) data. In addition, at each node, feature variables, *i.e.*, split features, are randomly selected and splitting is performed using these features one by one to find the best split. RF creates multiple trees; each tree is trained by using the bootstrapped samples. RF for regression is formed by growing trees on $(\boldsymbol{x}, y) \in D_m^*$ such that the predictions $\hat{f}(\boldsymbol{x})$ are numerical values as opposed to class labels in classification. OOB data is used for error calculation of the respective trees.

Suppose OOB data D_{OOB} of size N_{OOB} such that $(\boldsymbol{x}_j, y_j) \in D_{OOB}(j = 1, 2, \cdots, N_{OOB})$ and there are K_j trees that did not use sample $\boldsymbol{x}_j$ during their construction. Averaging predictions at $\boldsymbol{x}_j$ over K_j trees, the RF OOB prediction is derived:

$$\hat{f}_{OOB}(\boldsymbol{x}_j) = \frac{1}{K_j} \sum_{k=1}^{K} \hat{f}_k(\boldsymbol{x}_j) I[(\boldsymbol{x}_j, y_j) \in D_{OOB}] \quad \text{..... (22)}$$

where I (.) is the indicator function. The integrated mean-squared prediction error for $\hat{f}_{OOB}$ is

$$mspe[\hat{f}_{OOB}] = \frac{1}{N_{OOB}} \sum_{j=1}^{N_{OOB}} [y_j - \hat{f}_{OOB}(\boldsymbol{x}_j)]^2 \quad \text{..... (23)}$$

For validation data V of size N_v such that $(\boldsymbol{x}_v, y_v) \in V (v = 1, 2, \cdots, N_v)$, the RF prediction at $\boldsymbol{x}_v$ is the average prediction of K trees.

$$\hat{f}(\boldsymbol{x}_v) = \frac{1}{K} \sum_{k=1}^{K} \hat{f}_k(\boldsymbol{x}_v) \quad \text{..... (24)}$$

3.3. Model Validation

Finally, statistical models and gray-box models were con-

Table 1. Prediction results of TD temp through five models.

Modeling method	RMSE	r
First-principle model	2.72	0.77
Statistical model (PLS)	2.20	0.82
Statistical model (RF)	2.09	0.85
Gray-box model (PLS)	2.16	0.83
Gray-box model (RF)	1.73	0.89

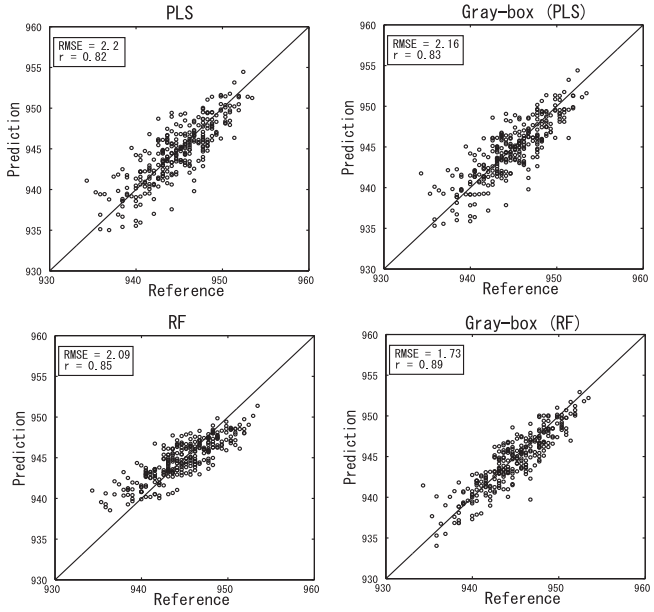

Fig. 6. Prediction of TD temp through PLS model, RF model, PLS-based gray-box model, and RF-based gray-box model.

structed and their prediction performance was compared by using real process data provided by Sumitomo Metal Industries, Ltd.

The number of samples was 1 444; 1 155 samples (80%) were used for modeling and the other 289 samples (20%) were used for validation. The prediction results of five models are summarized in **Table 1**. In addition, **Fig. 6** shows the prediction results through the statistical models, *i.e.*, PLS and RF, and the gray-box models that integrate the first-principle model with PLS and RF. The input variables of the statistical models were a total of 51 measured variables in the processes from the converter to the tundish.

The validation results show that the proposed gray-box models are superior to the first-principle model and the statistical models. Furthermore, the gray-box model combining the first-principle model and the RF model achieved the highest prediction accuracy. Its RMSE was 17% and 36% smaller than that of RF and the first-principle model, respectively. The results have clarified the advantage of the proposed gray-box model over other models. In particular, it is important that the prediction performance of the RF model alone was worse than the gray-box model, in which the RF model was used to estimate the prediction error of the first-principle model. Although RF can build a nonlinear process model, its direct application is not always the best approach.

By utilizing the ability of RF to calculate the importance of each input variable to the output variable, important input variables of the RF model integrated with the first-principle model were identified as shown in **Fig. 7**. The important

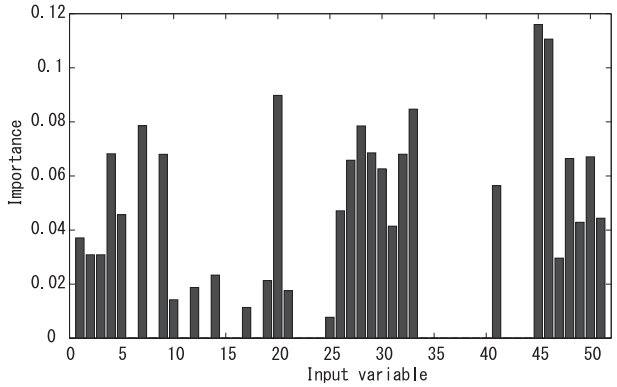

Fig. 7. Importance of input variables for RF model integrated with first-principle model in gray-box model.

variables, which contributed toward estimating the prediction error of the first-principle models, were the 20th, 33rd, 45th and 46th. The 20th variable is the amount of alloy added to the convertor, 33rd is the inlet temperature of the RH, 45th is the residence time of RH and 46th is the time duration from start of RH operation to the RH temp measurement. In other words, these four variables are crucial in describing the phenomena that cannot be modeled by the first-principle model.

4. Conclusions

In this study, a new gray-box model to predict the molten steel temperature in tundish (TD temp) in a steel making plant was proposed and was applied to the real process data. Partial least squares (PLS) and random forest (RF) were used to build statistical models. The results have clearly shown the advantage of the developed gray-box model over the first-principle model and the statistical models.

Acknowledgments

This study has been partially supported by the grant from ISIJ as an activity of research group, High Precision Process Control via Large Scale Database and Simulation Models, and also by Japan Society for the Promotion of Science (JSPS), Grant-in-Aid for Scientific Research (C) 21560793.

REFERENCES

1) M. Kano and Y. Nakagawa: *Comput. Chem. Eng.*, **32** (2008), 12.
2) A. Zoryk and P. M. Reid: *Iron Steelmaker*, **20** (1993), 21.
3) A. G. Belkovskii and Y. L. Kats: *Metallurgist*, **53** (2009), 261.
4) P. R. Austin, J. M. Camplin, J. Herbertson and I. J. Taggart: *ISIJ Int.*, **32** (1992), 196.
5) J. L. Xia and T. Ahokainen: *Metall. Mater. Trans. B*, **32** (2001), 733.
6) J. R. S. Zabadal, M. T. M. B. Vilhena and S. Q. B. Leit: *Ironmaking Steelmaking*, **31** (2004), 227.
7) T. Jormalainen and S. Louhenkilpi: *Steel Res. Int.*, **77** (2006), 472.
8) S. Sonoda, N. Murata, H. Hino, H. Kitada and M. Kano: *ISIJ Int.*, **52** (2012), 1086.
9) N. Gupta and S. Chandra: *ISIJ Int.*, **44** (2004), 15.
10) H. J. Odenthal, M. Javurek, M. Kirschen and N. Vogl: *Steel Res. Int.*, **81** (2010), 529.
11) M. Kano and K. Fujiwara: *J. Chem. Eng. Jpn.*, accepted.
12) B. Li, J. Morris and E. B. Martin: *Chemom. Intell. Lab. Syst.*, **64** (2002), 79.
13) M. Stone: *J. R. Stat. Soc. Ser. B. Stat. Methodol.*, **36** (1974), 111.
14) L. Breiman: *Mach. Learn.*, **45** (2001), 532.
15) T. K. Ho: Proc.the 3rd Int. Conf. on Document Analysis and Recognition, IEEE Computer Society Press, Los Alamitos, (1995), 278.
16) T. K. Ho: *IEEE Trnas. Pattern Anal. Mach. Intell.*, **20** (1998), 832.